does not appear to make predictions of a sign consistent with the photoemission and tunneling experiments.

[17]J. E. Houston, R. L. Park, and G. E. Laramore, Phys. Rev. Lett. 30, 846 (1973).

[18]The energy levels were obtained from *Atomic Energy Levels*, Natl. Bur. Stand. Circ. No. 467, edited by C. E. Moore (U.S. GPO, Washington, D.C., 1952), Vol. II. All the multiplet levels necessary for obtaining the average of configuration energies are tabulated, but the ^1S of the d^8s^2 configuration. This term was simply neglected in the configuration average.

[19]Ni^{2+} data are required here in addition to Ni and Ni^+. The tabulated (see Ref. 16) spectra for Ni^{2+} d^8 and d^7s is incomplete. Slater–Condon theory, taken with the observed levels, was used to place the centers of gravity of these configurations.

PHYSICAL REVIEW B VOLUME 8, NUMBER 2 15 JULY 1973

Electronic Structure of Vanadium Carbide

J. Zbasnik* and L. E. Toth†

University of Minnesota, Department of Chemical Engineering & Materials Science, Minneapolis, Minnesota 55455

(Received 2 January 1973)

The electronic structure of stoichiometric vanadium carbide has been computed using the augmented-plane-wave (APW) method and the energy bands for nonstoichiometric phases have been determined with the APW–virtual-crystal approximation. The energy bands exhibit a very strong dependence on the relative sizes of the assumed APW-sphere radii for vanadium and carbon. Bands for the nonstoichiometric phases show a marked deviation from a rigid-band behavior as the composition is varied. The results of x-ray-emission, heat-capacity, magnetic-susceptibility, and Hall-effect measurements are discussed in terms of the computed bands.

I. INTRODUCTION

Transition-metal carbides such as VC_{1-x} possess seemingly contradictory properties. These phases have several properties which indicate strong covalent bonds between carbon and the transition atom: for example, high melting points ranging to 3983 °C for TaC,[1] hardness values which lie between those of alumina and diamond,[2] and values of Young's modulus that are double those of the pure transition metals.[1] The electrical, magnetic, and optical properties of these phases, however, are often typically metallic and not much different from those of the parent transition metal.[1] In addition, nearly stoichiometric NbC, TaC, MoC, and WC are superconducting, with transition temperatures ranging from 10 to 14 K.[1]

Previous theories of the electronic structure and discussions of the relative importance of covalent and metallic bonding in carbides have been reviewed by Toth *et al.*[3] and Lye.[4] Several workers emphasized the importance of metal-metal bonding,[5–7] while others have declared that metal-nonmetal interactions are more important.[8,9] The latest band-structure calculations[10–14] and electron spectroscopy[15] and x-ray emission and absorption measurements[16] indicate that there is a mixture of metal-metal, metal-nonmetal, and possibly even ionic bonding.

In this paper, the electronic structures of stoichiometric and nonstoichiometric phases in the vanadium-carbon system are studied with the aid of augmented-plane-wave (APW) band-structure calculations. The calculations for the stoichiometric composition were performed using the perfect-crystal APW method due to Slater.[17] The band structures of several nonstoichiometric phases were computed using the augmented-plane-wave–virtual-crystal approximation (APW-VCA) method of Schoen.[18,19]

II. COMPUTATIONAL RESULTS AND DISCUSSIONS

A. APW Calculations for Stoichiometric VC

As a first step in the investigation of the energy bands of the vanadium-carbide system we calculated the band structure for stoichiometric VC with the NaCl crystal structure. VC phases can be prepared in the composition range from $VC_{0.88}$ to $VC_{0.65}$.[1,2] Even though stoichiometric VC does not exist, these calculations will be used as a starting point for the calculations on the nonstoichiometric phases.

In the APW scheme,[20–22] the one-electron crystal potential has a muffin-tin form; that is, the potential is spherically symmetric within spheres centered on the various atomic positions and constant in the interstitial volume. In each region, the potential is assumed to be the sum of two terms, one term which is purely electrostatic due to the nuclei and the charge density of all the electrons, and an exchange term. The Slater approximation was used for the exchange potential[23]:

$$V_x(r) = -6[(3/8\pi)p(r)]^{1/3},$$

where $p(r)$ is the total electronic charge density. The approximation has recently been examined by several authors[24–27] who have proposed that the calculations can be improved if the above potential is multiplied by a constant factor α, optimized according to a specific procedure ($X\alpha$ method). Schwarz[27] presents optimized α value for atoms H through Nb.

The present work on the V-C system was essentially completed before these optimized α values were published, so the full Slater potential, α equal to 1, was used. Neckel *et al.*[28] have recently published APW calculations for stoichiometric VC in which the full Slater exchange, as well as the $X\alpha$ exchange potential was used. These calculations show that the conclusions of this work would not be altered significantly by using the $X\alpha$ exchange potential.

The starting potential was computed according to the procedure described by Mattheiss.[29] In this procedure, the charge densities and the corresponding electrostatic potentials of the constituent atoms, as computed, for example, by Herman and Skillman,[30] are used. The electrostatic contribution to the potential inside the APW spheres is obtained by superposing the free-atom electrostatic potentials using Löwdin's α-function expansion[31] and retaining only the spherically symmetric terms The exchange contribution is determined by inserting the superposed charge density into the above equation. In the $X\alpha$ method, this exchange term would be multiplied by the factor α, depending upon the type of atom residing on the site. The electrostatic contribution to the potential in the constant-potential region is the arithmetic average of the potential over the interstitial volume, and the exchange term is computed from the average charge density in the region. In the $X\alpha$ method, this exchange term would be multiplied by $\frac{2}{3}$, the factor for free electrons determined by Kohn and Sham[32] and Gaspar[33] using a variational calculation.

At the present time, there are no clearcut guidelines to assist in the choice of proper APW-sphere radii when the crystal contains more than one type of atom. To assess the dependence of the computed energy bands on the sphere radii, two potentials, corresponding to the APW-sphere radius ratio R_C/R_V values of 0.576 and 0.65, were constructed. The potentials are designed as VC*P*1 and VC*P*2, respectively. The first value, 0.576, corresponds to the radius ratio one would obtain by using Pauling radii for V with a coordination number of 12 and a value for C appropriate for a coordination number of 1 and the second value, 0.65, corresponds to both atoms having a coordination number of 12.[34] The lattice parameter was taken to be 4.182 Å (7.902 a.u.), a value obtained from Pearson's compilation[35] and which can be seen to be an extrapolation of the observed lattice parameters to the stoichiometric composition.[2] The potential inside the APW spheres is unaffected by the values of sphere radii—only the value of the potential in the interstitial region, and hence the discontinuities on the sphere boundaries, are affected.

The choice of the values for the radius ratio R_C/R_V was somewhat arbitrary. It is generally accepted, however, on the basis of crystallographic evidence, that R_C/R_V must lie between 0.41 and 0.73, or in the general range for stability of the NaCl structure. This range has been derived by considering ionic compounds; crystallographic instability occurs when like ions come into direct contact. The NaCl structure (coordination number 6) becomes unstable when anions come into direct contact or if $R_c/R_a \leq 0.41$, where c and a refer to cation and anion, respectively. The upper limit is obtained by considering the CsCl structure with the coordination number of 8. This structure becomes unstable when $R_c/R_a \leq 0.73$. Thus for stability of the NaCl structure the radius ratio should lie between 0.41 and 0.73. For transition-metal carbides, this range is valid even though the degree of ionic bonding is probably small (see Ref. 1 for a more complete discussion). Values of the radius ratio chosen for previous APW calculations on carbides have all been outside this range. The general agreement between this result and those of Neckel *et al.*[28] (radius ratio = 0.9) indicates that carrying the calculation to self-consistency removes much of the dependency of the eigenvalues on the assumed sphere radii. In our calculation the value of 0.65 was arbitrarily chosen for the self-consistent calculations.

The potentials were fed into the symmetrized version of the APW program and the one-electron eigenvalues determined. Using the notation of Bouckaert, Smoluchowski, and Wigner,[36] the eigenvalues were determined for the states Γ, X, W, L, K, Q, Z, $\Delta(0,0,1)$, $\Delta(0,0,2)$, $\Delta(0,0,3)$, $\Sigma(0,1,1)$, $\Sigma(0,2,2)$, and $\Delta(1,1,1)$, where the numbers in parentheses are the wave vectors expressed in units of $\pi/2a$. In addition, the eigenvalues for the states (0, 2, 3), (0, 1, 2), (0, 1, 3), (1, 2, 2), (1, 2, 1), and (1, 1, 3), also in units of $\pi/2a$, were obtained by interpolating between the calculated values. This is equivalent to considering 256 points in the full Brillouin zone. The magnitude of the highest wave vector used in the expansion was $\pi/a(80)^{1/2}$, sufficient to ensure that all the states will converge to 0.005 Ry.[21] These results are presented in the $E(k)$ curves, Figs. 1 and 2. The Fermi level is determined by arranging the eigenvalues in order of increasing energy and filling them with the proper number of electrons. Also shown are the corresponding density-of-states curves which were

obtained from the eigenvalues for the 256 states. The histogram-averaging procedure of Snow and Waber[37] was used. Although a better method to obtain the density-of-states curve is to fit the APW eigenvalues to a model Hamiltonian and then recalculate the eigenvalues on a finer mesh in k space, the agreement that Neckel[28] obtains between the density of states computed from the APW eigenvalues and that from the model Hamiltonian indicates that the present procedure should be adequate for the purpose at hand. $N(E)$ curves for the higher-lying states were not determined because these eigenvalues were incompletely known.

To assist in the understanding of the $E(k)$ and density-of-state curves, the wave functions for the states Γ, X, W, L, $\Delta(0,0,1)$, and $\Sigma(0,1,1)$, where the numbers in parentheses are the wave vectors expressed in units of π/a, were analyzed using the procedure outlined by Mattheiss *et al.*[21] One obtains from this analysis Q_{out}, the fraction of the normalization in the interstitial volume for the state, and $Q_{s,l}$, the fraction of the normalization that can be accounted for by considering the volume of the sth-type sphere and the APW basis function corresponding to angular momentum l. The results of this analysis are given in Table I for the two potentials.

The charge analysis for representative states in the lowest-lying energy band for potential VCP1 reveals that a significant amount of the normalization occurs in the carbon spheres with $l=0$. These states can then be considered as being derived principally from the carbon 2s atomic levels. The states in the next-higher set of bands have most of the charge located on the carbon sites with $l=1$ and can therefore be associated with the carbon 2p atomic levels. The states in the next-higher-lying bands are concentrated in the vanadium spheres with $l=2$ and can be classified as metal 3d states. The vanadium 4s states lie above this 3d band.

For potential VCP2, the lowest-lying states again can be classified as carbon 2s states on the basis of the charge analysis. However, the states which are classified as carbon 2p states for VCP1 are now mixed with 3d states from the metal atoms. The 2p-3d interaction is revealed in the charge analysis; the amount of charge associated with angular momentum $l=1$ in the carbon spheres is approximately equal to the charge with $l=2$ on the vanadium sites. The 4s band lies above this 3d-2p hybrid band.

The bonding schemes that can be inferred from these two calculations differ vastly. For VCP1, the potential corresponding to the smaller carbon sphere, there is only indirect vanadium-carbon in-

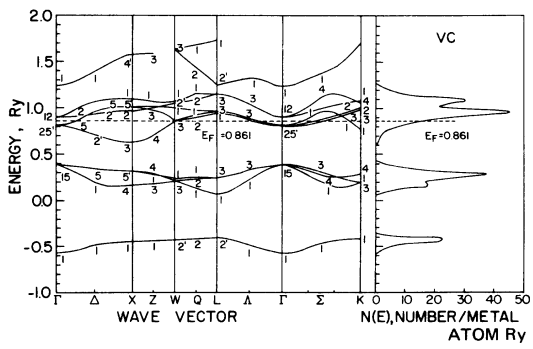

FIG. 1. Non-self-consistent band structure for VC assuming an APW sphere radius ratio R_C/R_V of 0.576.

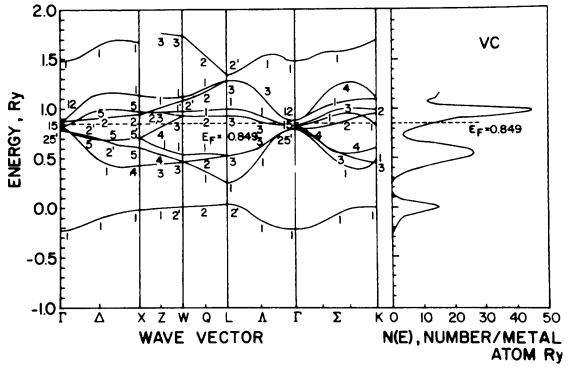

FIG. 2. Non-self-consistent band structure for VC assuming an APW sphere radius ratio R_C/R_V of 0.65.

TABLE I. APW charge analysis (in %) of the occupied states for potentials VCP1 and VCP2.

		VCP1			VCP2	
State	Out	V sphere	C sphere	Out	V sphere	C sphere
Γ_1	29.2	19.1 $l=0$	50.6 $l=0$	36.0	22.8 $l=0$	40.8 $l=0$
Γ_{15}	21.4	•••	67.1 $l=1$	21.6	•••	67.1 $l=1$
$\Gamma_{25'}$	10.6	88.0 $l=2$	•••	12.0	86.8 $l=2$	•••
Δ_1	26.8	9.7 $l=0$	54.6 $l=0$	32.7	13.5 $l=0$	44.8 $l=0$
					5.0 $l=1$	
	25.4	5.1 $l=0$	47.5 $l=1$			
		16.1 $l=2$	•••	25.0	31.6 $l=2$	32.9 $l=1$
Δ_5	23.4	6.8 $l=1$	60.1 $l=1$	22.8	6.5 $l=1$	39.5 $l=1$
					27.8 $l=2$	
$\Delta_{2'}$	19.8	78.4 $l=2$	•••	21.4	76.9 $l=2$	•••
X_1	23.6	14.2 $l=2$	59.2 $l=0$	24.5	20.1 $l=2$	52.2 $l=0$
X_3	24.8	73.9 $l=2$	•••	26.8	71.8 $l=2$	•••
$X_{4'}$	31.5	21.4 $l=1$	46.5 $l=1$	40.6	24.1 $l=1$	35.1 $l=1$
X_5	24.2	10.4 $l=1$	60.3 $l=1$	27.3	12.8 $l=1$	55.6 $l=1$
W_1	23.2	6.7 $l=1$	52.6 $l=1$	22.9	7.4 $l=0$	38.7 $l=1$
		14.6 $l=2$	•••		28.9 $l=2$	•••
W_3	29.2	16.0 $l=1$	47.9 $l=1$	36.2	15.7 $l=1$	29.5 $l=1$
		5.4 $l=2$	•••		18.0 $l=2$	•••
$W_{2'}$	23.3	3.8 $l=1$	60.4 $l=0$	24.2	4.1 $l=1$	54.4 $l=0$
		11.0 $l=2$	•••		16.4 $l=2$	
L_1	30.7	17.7 $l=0$	40.4 $l=1$	37.5	17.1 $l=0$	26.1 $l=1$
		10.4 $l=2$	•••		19.1 $l=2$	
$L_{2'}$	24.5	12.3 $l=1$	60.2 $l=0$	28.5	14.6 $l=1$	54.9 $l=0$
L_3	21.4	25.9 $l=2$	51.3 $l=1$	19.1	46.9 $l=2$	33.3 $l=1$
Σ_1	25.0	8.3 $l=1$	58.1 $l=0$	29.5	9.7 $l=1$	49.5 $l=0$
	27.7	11.5 $l=0$	44.5 $l=1$	29.8	9.8 $l=0$	29.3 $l=1$
		12.9 $l=2$	•••		26.0 $l=2$	
Σ_3	27.2	11.2 $l=1$	49.9 $l=1$	32.1	10.5 $l=1$	27.6 $l=1$
		9.2 $l=2$			28.7 $l=2$	
Σ_4	21.2	23.4 $l=2$	53.0 $l=1$	18.6	43.7 $l=2$	36.0 $l=1$

teraction; most of the bonding is due to metal-metal and carbon-carbon interacting. Several theories emphasizing the importance of this type of bonding for transition-metal carbides have been proposed.[5-7] On the other hand, the results for VC$P2$ suggest that the primary bonding is between the $3d$ vanadium states and the $2p$ carbon states. This type of bonding has also been proposed, based on band-structure calculations,[8-14] electron spectroscopy,[15] and x-ray emission and absorption measurements.[16]

B. Self-Consistent APW Calculations for Stoichiometric VC

The results of the calculation for the potential VC$P2$ were used as the starting point for the self-consistent calculation. Herman–Skillman[30] charge densities for the $3p$ and lower levels were summed to obtain the core charge density for the vanadium sphere and in the carbon sphere the core was formed from the Herman–Skillman charge density for the $1s$ state. The APW valence charge density was obtained by averaging the radial charge density over the occupied states at Γ, X, L, and W in the full zone. The charge density was computed according to the method of Mattheiss, Wood, and Switendick[21] and the averaging was performed using the procedure described by Euwema *et al.*[38] This APW charge density was used, along with the core densities, to construct a new potential in the manner described by Mattheiss, Wood, and Switendick.[21] The APW eigenvalues at these points for this new potential were compared with the previously determined eigenvalues. If any of the eigenvalues changed by more than 0.002 Ry, a new potential was constructed and the process repeated.

The energy bands and the density-of-states curve for this approximately self-consistent potential are shown in Fig. 3. The results of a charge analysis for the occupied states at the equivalent of 32 points in the full Brillouin zone are listed in Table II.

By iterating the calculation, the carbon-derived states are elevated and those from the metal are depressed in energy, indicating that in the superposition procedure the carbon spheres contained too much charge and the vanadium too little. The self-consistent bands have 4.23 electrons in the V sphere and 2.50 in the C sphere, compared to 3.44 electrons in V and 3.18 in C for potential VC$P2$. When the present energy bands are compared to those of Neckel and co-workers,[28] redrawn to conform to the noncrossing rule of group theory, it is observed that the two bands are almost identical. The $2s$ bands have the same width of 0.27 Ry. Our $3d$-$2p$ band is 0.04 Ry narrower than Neckel's, 0.98 Ry as compared to 1.02 Ry. The spacing between the lower $2s$ band and the upper $3d$-$2p$ band for the two calculations differ by only 0.01 Ry. Potorocha *et al.*[14] used a tight-binding method and obtained energy bands which are in qualitative agreement with the APW results but differ in the ordering of the eigenvalues. Disagreement is found with the energy bands of Lye and co-workers,[7] who propose that both metal and carbon s states are located below the Fermi level and metal and carbon p states are above.

The charge analysis yields some interesting information about the electronic structure of the system. About 50% of the charge for the states in the lowest-lying band is in the carbon spheres, with the remainder shared nearly equally between the vanadium spheres and the interstitial volume. The

TABLE II. APW charge analysis (in %) of the occupied states for self-consistent vandium carbide.

State	Outside	V sphere	C sphere
Γ_1	37.7	24.4 $l=0$	37.6 $l=0$
$\Gamma_{25'}$	10.6	88.4 $l=2$	•••
Γ_{12}	4.6	94.1 $l=2$	•••
$\Delta_1(0, 0, 1)$	34.5	14.9 $l=0$	41.0 $l=0$
		5.3 $l=1$	
	23.1	41.4 $l=2$	26.2 $l=1$
$\Delta_{2'}(0, 0, 1)$	19.0	79.6 $l=2$	•••
$\Delta_5(0, 0, 1)$	18.1	53.8 $l=2$	21.2 $l=1$
X_1	24.8	23.8 $l=2$	48.0 $l=0$
$X_{4'}$	43.0	25.6 $l=1$	31.2 $l=1$
X_3	24.2	74.6 $l=2$	•••
$X_{5'}$	29.0	14.3 $l=1$	52.2 $l=1$
W_1	20.7	6.8 $l=0$	30.5 $l=1$
		40.2 $l=2$	
$W_{2'}$	24.5	20.0 $l=2$	50.3 $l=0$
W_3	35.6	14.6 $l=1$	21.9 $l=1$
		27.3 $l=2$	
L_1	37.4	16.8 $l=0$	21.6 $l=1$
		24.0 $l=2$	
L_3	17.1	57.7 $l=2$	24.7 $l=1$
$L_{2'}$	30.3	16.2 $l=1$	51.7 $l=0$
$\Sigma_1(0, 1, 1)$	31.5	10.1 $l=1$	45.6 $l=0$
	28.3	8.8 $l=0$	23.2 $l=1$
		34.5 $l=2$	
$\Sigma_3(0, 1, 1)$	30.6	40.1 $l=2$	19.0 $l=1$
$\Sigma_4(0, 1, 1)$	16.3	55.1 $l=2$	27.0 $l=1$
$\Sigma_2(0, 1, 1)$	6.1	93.1 $l=2$	•••

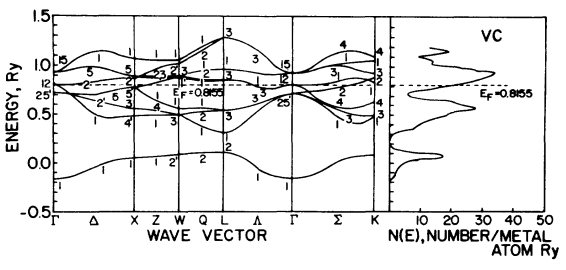

FIG. 3. Self-consistent band structure for VC assuming an APW sphere radius ratio R_C/R_V of 0.65.

charge on the vanadium sites has d- as well as s-type symmetry, which can be construed to be some small amount of s-d bonding. The analysis of the states in the $2p$-$3d$ bands again points to the interaction between p and d electrons. The states in the Σ_2 band, and possibly also in Δ_2 and Δ_3, appear to be nearly pure d-type states. Thus, we arrive at the conclusion that the strong bonding is caused by covalent-overlap interactions below the Fermi surface, while a significant amount of the states near the Fermi level are d type so that certain properties will be metallic in nature.

C. APW-VCA Calculations for Nonstoichiometric VC

The electronic structure of nonstoichiometric VC was computed using Schoen's APW-VCA method.[18,19] This method was derived by using Lloyd's[39] APW pseudopotential in the momentum representation for an APW sphere centered at $\vec{l}$ and summing over all the lattice sites. Schoen[18,19] performed this sum for a random alloy, and the resulting secular equation is the same as the corresponding APW equation for a perfect crystal, except that the logarithmic derivative of a particular site in the unit cell is replaced by the average of the logarithmic derivatives of the atomic species that can occupy the site.

In the nonstoichiometric V-C system we have assumed that the phases are composed of three types of atoms: vanadium atoms, carbon atoms, and vacancies. Although carbon ordering has been observed for V_8C_7 and V_6C_5,[1] we will assume that the vacancies are randomly distributed on the carbon sublattice. Schoen and Denker[40] have applied the APW-VCA method to the Ti-O system. They constructed a virtual-crystal-type potential for the Ti and O spheres and assumed that the potential in a sphere occupied by a vacancy was a constant, equal to zero. In the present work we have assumed that the potentials in the V and C spheres are the respective self-consistent potentials and the potential in a vacancy sphere is equal to zero. Unfortunately, as Schoen[18,19] has pointed out, the APW-VCA method cannot be iterated to self-consistency as was done for the stoichiometric case. The appropriateness of the potential must be judged by the degree to which the bands can be correlated with experimental results. The potentials employed here probably overestimate the potentials in both V and C spheres, so that all the eigenvalues would be shifted slightly upward if a more accurate potential were used. We have also neglected any change of lattice parameter with composition, since the observed lattice parameters vary by only 1% over the entire composition range.[1,2]

The $E(k)$ curves for the compositions $VC_{0.9}$, $VC_{0.8}$, and $VC_{0.7}$ are shown in Figs. 4–6. Apart from a continuous distortion of the bands as the carbon concentration is changed, the bands for the nonstoichiometric phases are qualitatively similar to the bands obtained for stoichiometric VC, Fig. 3. No new bands arising from vacancy states were detected in the energy range studied. All of the carbon states and states which represent metal-carbon interactions are elevated in energy as the carbon is removed, while the bands which are composed of localized d states, Δ_2', Δ_2, Λ_3 from Γ_{12} and Σ_2 from $\Gamma_{25'}$, are not affected by changing the carbon concentration. Because of the similarity between the stoichiometric and the nonstoichiometric bands, the previously proposed bonding scheme can be assumed to be valid for the nonstoichiometric phases.

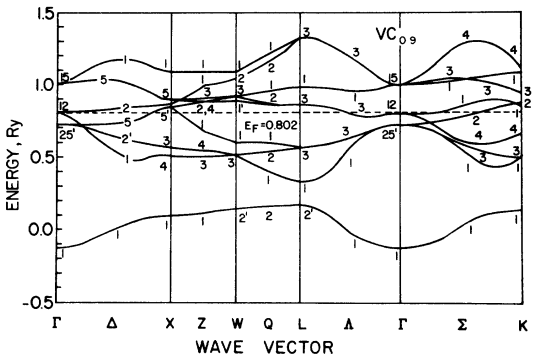

FIG. 4. APW-VCA energy bands for $VC_{0.9}$.

Schoen[18] has emphasized that the construction of the density-of-states curve for the APW-VCA bands is more complicated than for a perfect crystal because when these APW-VCA states are counted they must be weighted according to the concentration of atomic levels from which they coalesced. The density-of-states curves for the nonstoichiometric phases are shown in Fig. 7. In obtaining these curves, it was assumed that the vacancies could interact with all the states and a perfect-crystal counting scheme was used. The lowest band, due primarily to carbon $2s$ and vacancy states, is constantly elevated in energy as the carbon concentration is reduced, its shape remaining approximately constant. The widths of the higher-lying d bands, responsible for the peaks at approximately 0.6 and 0.85 Ry, decrease with decreasing carbon concentration, and the entire structure is altered significantly.

III. COMPARISON WITH EXPERIMENTAL DATA

A. Soft X-Ray Emission

Fischer[16] has reported the vanadium $L_{II,III}$ x-ray emission and absorption spectra for VC, in which photons due to electronic transitions to a final V-$2p$ core state are measured. Based on calculations of the transition probability for dipole

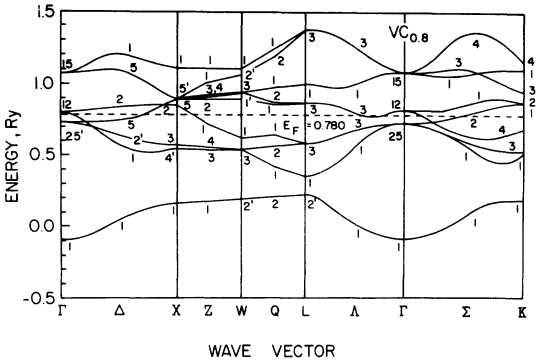

FIG. 5. APW-VCA energy bands for $VC_{0.8}$.

transitions,[41] it is expected that the emission spectrum will be determined by the density-of-states curves for states that have a significant $l=0$ or $l=2$ charge component in the vanadium sphere. The carbon K emission band for VC, caused by electronic transitions to vacant $1s$ carbon levels, has been measured by Holliday.[42] Here, the emission spectrum should be dominated by transitions from valence states that have a significant $l=1$ component in the sphere.

Although the transition probabilities as well as the density of states are needed to explain the shape of the emission spectra, gross features such as band spacings and widths should be explainable in terms of the density-of-states curve. In Fig. 8 we have reproduced and superimposed the x-ray spectra obtained by Fischer[16] and Holliday[42] along with the density-of-states curve for $VC_{0.9}$, the most nearly stoichiometric composition that has been prepared.[1,2]

The main peak in Fischer's emission spectrum is attributed to transitions from the states which have a significant amount of $l=2$ charge in the vanadium sphere. The structure on the high-energy side of this peak can be roughly correlated with the structure in the density-of-states curve. The next-

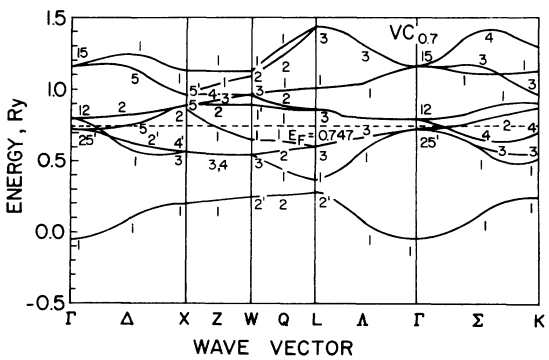

FIG. 6. APW-VCA energy bands for $VC_{0.7}$.

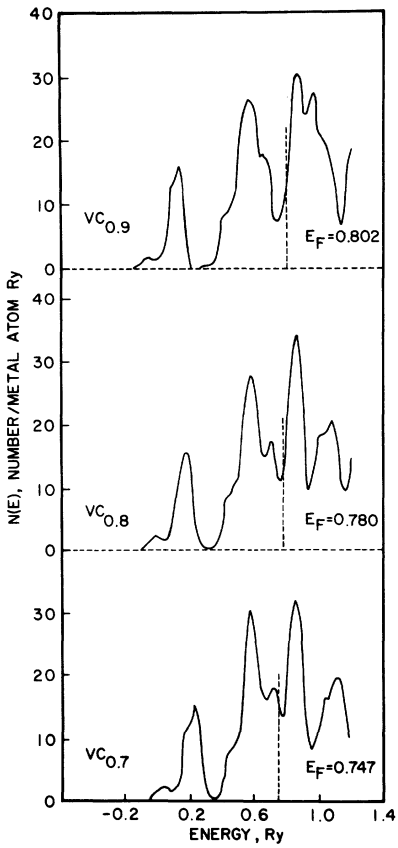

FIG. 7. Density-of-states curves for VC_x phases.

lower emission band can be correlated with the $2s$ band on the density-of-states curve, because these states have some $l=0$ charge component in the vanadium sphere. Fischer's lowest band, which may be a plasmon satellite of the main peak, cannot be correlated with the computed band structure. The main peak in Holliday's C K emission spectrum is attributed to transitions from states in the $2p$-$3d$ band because of the presence of a $l=1$ charge component in the carbon spheres.

B. Electronic Specific Heats

N_γ, the heat-capacity density of states, is computed from γ, the measured electronic specific-heat coefficient, by

$$N_\gamma = (3/2\pi^2 k_B^2)\gamma ,$$

where k_B is Boltzmann's constant and N_γ is the density of states for a single spin direction. If the electronic system is noninteracting, N_γ will be equal to $N(0)$, the density of states at the Fermi level obtained from a band-structure calculation. In most systems the electrons will experience interactions, so N_γ will be larger than $N(0)$. Migdal[43] has shown that the relation between these two quantities can be expressed as

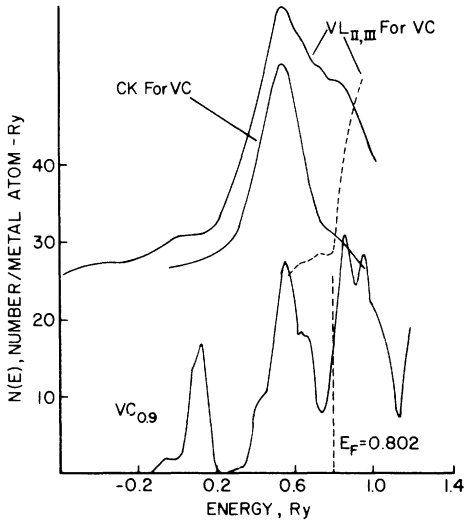

FIG. 8. Comparison of the computed density of states for $VC_{0.9}$ with $VL_{II,III}$ x-ray data due to Fischer (Ref. 16) and CK x-ray emission data of Holliday (Ref. 42) for VC. The dashed line is Fischer's (Ref. 16) absorption curve.

$$N(0) = N_\gamma/[1 + N(0)V_p] ,$$

where V_p is a parameter representing the interaction. Often the interaction parameter will be small so that the measured values will be roughly proportional to the band-structure density of states at the Fermi level.

Ishikawa[44] and Ishikawa and Toth[45] have measured the electronic specific heats of several VC_x phases. The heat-capacity density-of-states values N_γ, as well as the values obtained from the present calculation, $N(0)$, are plotted in Fig. 9. The heat-capacity measurements of Lowndes *et al.*[46] are in agreement with these results, with the exception that a more pronounced peak at high carbon concentrations is found.

Using Migdal's formula to compute a value for V_p and substituting this value, as well as the Debye temperature of 685 K,[44,45] into McMillan's formula for the superconducting transition temperature,[47]

$$T_c = \frac{\Theta_D}{1.45} \exp - \frac{1.04[1 + N(0)V_p]}{N(0)V_p - 0.13[1 + 0.62N(0)V_p]} ,$$

a value for $T_c \approx 10^{-12}$ K was computed. Several workers[48,49] have failed to find superconductivity in VC_x phases above 30 mK. The reverse of this type of analysis was performed for pure V, which has a T_c of about 5.0 K, and it was found that the parameter V_p for $VC_{0.9}$ is only about 25% less than that for vanadium. The main reason for the absence of superconductivity in the VC system is that the $N(0)$ values are less than half for those of vanadium.

C. Magnetic Susceptibility

Ishikawa,[44] Ishikawa and Toth,[45] and Bloom *et al.*[50] have measured the magnetic susceptibility of VC_x phases. The specimens were paramagnetic and exhibited extremely high values of χ. The curve labeled N_χ in Fig. 9 represents density-of-states values calculated by assuming that the entire susceptibility was due to Pauli-spin paramagnetism. The large difference between these N_χ values and those for N_γ and $N(0)$ was attributed to an orbital paramagnetic contribution to the susceptibility that increases as the carbon concentration is decreased.

Orbital paramagnetic susceptibility varies inversely with bandwidth and depends on the position of the Fermi level in the band.[51] The widths of the computed alloy bands shown in Fig. 7 decrease as the carbon concentration is reduced and presumably would yield an increasing orbital paramagnetic contribution. Since the d bandwidths of the VC_x phases are larger than the bandwidth of approximately 0.15 Ry computed for vanadium,[52] the orbital paramagnetic susceptibility for the carbides should be less than the value of 75×10^{-6} emu/mole computed for pure V.[53] Values that are needed to bring the N_χ in better agreement with N_γ and $N(0)$ range from approximately 66×10^{-6} emu/mole for $VC_{0.7}$ to zero for the highest carbon concentrations. Bloom and co-workers[50] have discussed the orbital paramagnetic susceptibility of VC_x based on composition-independent energy bands of Lye *et al.*[7] The present bands do not allow such an interpretation.

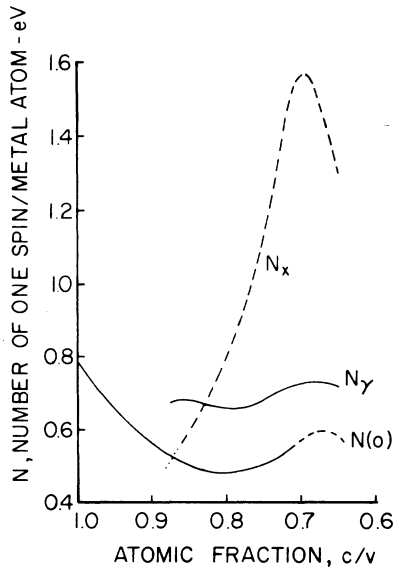

FIG. 9. Comparison of the computed Fermi-level density of states $N(0)$ with the values determined from the electronic specific heat N_γ and the magnetic susceptibility N_χ, by Ishikawa and Toth (Ref. 45).

D. Hall Coefficients

The low-temperature Hall constants as reported by Borukhovich *et al.*[54] monotonically increase from a negative value for $VC_{0.88}$ to a positive value for $VC_{0.72}$, passing through zero at a composition of about $VC_{0.8}$.

Although a calculation of the Hall constants would be extremely complicated, the observed behavior can be rationalized with the computed band structures. At the highest carbon concentration the Fermi level lies on a rising portion of the density-of-states curve, which indicates that a new band is being filled, resulting in a dominance of electronic conduction and a correspondingly negative Hall constant. At a composition with slightly less carbon than $VC_{0.8}$, the Fermi level lies in a minimum of the density-of-states curve and the electronic and hole contributions cancel. Decreasing the carbon concentration still more results in the Fermi level lying in a falling portion of the density-of-states curve and hole conduction predominating.

ACKNOWLEDGMENTS

The calculations were performed at the University of Minnesota Computer Center. The authors are indebted to Dr. J. M. Schoen for providing them with a copy of the APW programs.

---

*Present address: Inst. f. Physik. Chemie, 44 Munster, W. Germany.

†Research supported by a grant from the National Science Foundation.

[1]L. E. Toth, *Transition Metal Carbides and Nitrides* (Academic, New York, 1971).
[2]E. K. Storms, *The Refractory Carbides* (Academic, New York, 1967).
[3]L. E. Toth, J. Zbasnik, Y. Sato, and W. Gardner, in *Anisotropy in Single-Crystal Refractory Compounds*, edited by F. W. Vahldiek and S. A. Mersol (Plenum, New York, 1968), p. 249.
[4]R. G. Lye, in *Atomic and Electronic Structure of Metals* (American Society for Metals, Metals Park, Ohio, 1967), p. 99.
[5]R. Kiessling, Metall. Rev. 2, 77 (1957).
[6]P. Costa and R. R. Conte, Nucl. Met. AIME **10,** 3 (1964).
[7]R. G. Lye, G. E. Hollox, and J. D. Venables, in Ref. 3, Vol. 2, p. 445.
[8]R. E. Rundle, Acta Crystallogr. **1,** 180 (1948).
[9]H. Bilz, Z. Phys. **153,** 338 (1958).
[10]V. Ern and A. C. Switendick, Phys. Rev. **137,** 1927 (1965).
[11]R. G. Lye and E. M. Logothetis, Phys. Rev. **147,** 622 (1966).
[12]J. B. Conklin, Jr. and D. J. Silversmith, Int. J. Quantum Chem. Symp. **2,** 243 (1968).
[13]K. Schwarz and J. B. Conklin, Jr., Bull. Am. Phys. Soc. **15,** 310 (1970).
[14]V. I. Potorocha, V. A. Tskhai, and P. V. Geld, Phys. Status Solidi B **48,** 119 (1971).
[15]L. Ramqvist, J. Appl. Phys. **42,** 2113 (1971).
[16]D. W. Fischer, J. Appl. Phys. **40,** 4151 (1969).
[17]J. C. Slater, Phys. Rev. **51,** 846 (1937).
[18]J. M. Schoen, Phys. Rev. **184,** 858 (1969).
[19]J. M. Schoen, Ph.D. thesis (Columbia University, 1969) (unpublished).
[20]T. Loucks, *Augmented Plane Wave Method* (Benjamin, New York, 1967).
[21]L. F. Mattheiss, J. H. Wood, and A. C. Switendick, in *Methods in Computational Physics*, edited by B. Alder, S. Fernbach, and M. Rotenberg (Academic, New York, 1968), p. 64.
[22]J. O. Dimmock, in *Solid State Physics*, edited by H. Ehrenreich, F. Seitz, and D. Turnbull (Academic, New York, 1971), Vol. 26, p. 104.
[23]J. C. Slater, Phys. Rev. **81,** 385 (1951).
[24]J. C. Slater and J. H. Wood, Int. J. Quantum Chem. **4,** 3 (1971).
[25]J. C. Slater and K. H. Johnson, Phys. Rev. B **5,** 844 (1972).
[26]I. Lindgren and K. Schwarz, Phys. Rev. A **5,** 542 (1972).
[27]K. Schwarz, Phys. Rev. B **5,** 2466 (1972).
[28]A. Neckel, P. Rastl, P. Weinberger, and Renate Mechter, Theor. Chim. Acta **24,** 170 (1972).
[29]L. F. Mattheiss, Phys. Rev. **133,** 1399 (1964).
[30]F. Herman and S. Skillman, *Atomic Structure Calculations* (Prentice-Hall, Englewood Cliffs, N.J., 1963).
[31]P. O. Löwdin, Adv. Phys. **5,** 1 (1956).
[32]W. Kohn and L. J. Sham, Phys. Rev. **145,** 561 (1966).
[33]R. Gaspar, Acta Phys. Hung. **3,** 263 (1954).
[34]L. S. Darken and R. W. Gurry, *Physical Chemistry of Metals* (McGraw-Hill, New York, 1953), p. 61.
[35]W. B. Pearson, *A Handbook of Lattice Spacings and Structures of Metals and Alloys* (Pergamon, New York, 1964), p. 963.
[36]L. P. Bouckaert, R. Smoluchowski, and E. Wigner, Phys. Rev. **50,** 58 (1936).
[37]E. C. Snow and J. T. Waber, Phys. Rev. **157,** 570 (1967).
[38]R. N. Euwema, D. J. Stukel, T. C. Collins, J. S. DeWitt, and D. J. Shamkland, Phys. Rev. **178,** 1419 (1969).
[39]P. Lloyd, Proc. Phys. Soc. Lond. **86,** 825 (1965).
[40]J. M. Schoen and S. P. Denker, Phys. Rev. **184,** 864 (1969).
[41]J. C. Slater, *Quantum Theory of Atomic Structure* (McGraw-Hill, New York, 1960), Vol. II, p. 222.
[42]J. E. Holliday, in *Soft X-Ray Band Spectra*, edited by D. J. Fabian (Academic, New York, 1968), p. 101.
[43]A. B. Migdal, Zh. Eksp. Teor. Fiz. **34,** 1438 (1958) [Sov. Phys.-JETP **7,** 996 (1958)].
[44]M. Ishikawa, Ph.D. thesis (University of Minnesota, 1970) (unpublished).
[45]M. Ishikawa and L. E. Toth, Monatsh. Chem. **103,** 492 (1972).
[46]D. H. Lowndes, Jr., H. Finegold, and R. G. Lye, Philos. Mag. **21,** 245 (1970).
[47]W. L. McMillan, Phys. Rev. **167,** 331 (1968).
[48]N. Pessall, J. K. Hulm, and M. S. Walker, Westinghouse Research Laboratories, Final Rept. No. AF 33 (615) - 2729, 1967 (unpublished).
[49]D. W. Bloom, L. Finegold, R. G. Lye, R. Radebaugh, and J. D. Siegwarth, Phys. Lett. A **33,** 137 (1970).
[50]D. W. Bloom, L. Finegold, A. Tveten, and R. G. Lye, Philos. Mag. **24,** 603 (1971).
[51]R. Kubo and Y. Obata, J. Phys. Soc. Jap. **11,** 547 (1956).
[52]D. A. Papaconstantopoulos, J. R. Anderson, and J. W. McCaffrey, Phys. Rev. B **5,** 1214 (1972).
[53]M. Yasui and M. Shimizu, J. Phys. Soc. Jap. **31,** 378 (1971).
[54]A. S. Borukhovich, P. V. Geld, V. A. Tskhai, L. B. Dubrovskaya, and I. I. Matveenko, Phys. Status Solidi B **45,** 179 (1971).